Applied Energy 140 (2015) 161–170

Contents lists available at ScienceDirect

Applied Energy

journal homepage: www.elsevier.com/locate/apenergy

Rankine cycle efficiency gain using thermoelectric heat pumps

J. Siviter *, A. Montecucco, A.R. Knox

School of Engineering, Rankine Building, University of Glasgow, Glasgow G12 8LT, United Kingdom

HIGHLIGHTS

- Rankine cycle electrical power plant fuel load reduced by over 1.5
- Thermoelectric heat pumps are used to increase the efficiency of the Rankine cycle.
- We scavenge the enthalpy released in the condenser for preheating the return water.
- We measure with a new test rig the optimum COP for maximum efficiency increase.
- We show a cost-benefit analysis of applying the system to a thermal power plant.

ARTICLE INFO

Article history:
Received 15 July 2014
Received in revised form 9 September 2014
Accepted 29 November 2014
Available online 17 December 2014

Keywords:
Rankine cycle
Thermal power plant cycle efficiency
Thermoelectric
Heat pumping

ABSTRACT

The Rankine cycle remains the dominant method of thermal plant electricity generation in the world today. The cycle was described over 150 years ago and significant performance advances continue to be realised. On-going metallurgy research has enabled the operating pressure and temperature of the boiler and turbine to be increased, thereby improving the cycle efficiency. The ubiquitous use of the Rankine cycle on a massive scale in conjunction with fossil fuels as the energy source continues to motivate further efficiency improvements in the cycle.

Previous work established a theoretical basis for the use of thermoelectric heat pumps (THPs) in the condensation process of the Rankine cycle to positively impact cycle efficiency. The work presented here experimentally validates this prior work and provides performance metrics for current commercially available THPs and quantifies how their use can increase the efficiency of the Rankine cycle as implemented in a large power plant.

A commercial THP is characterised to obtain its Coefficient of Performance (COP) variation with input current and the amount of thermal energy transported. A larger-scale system comprising of a multistage thermoelectric heat pump is then considered, demonstrating that using commonly available THPs a fuel load reduction of over 1.5% is achievable for a typical 600 MW_e generating set whilst simultaneously increasing the overall plant cycle efficiency from 44.9% to 45.05%.

The paper concludes with a cost-benefit analysis of the system, showing that over a four year period the saving in fuel used can easily re-coup the capital cost incurred by the addition of the condenser heat pump.

1. Introduction

Globally, Rankine-cycle based power plants are the dominant means of electrical power generation. Large thermal power plants utilise high pressure and temperature steam to maximise the thermal to electrical energy conversion with, for modern plant, a cycle efficiency approaching 50% [1]. However, the majority of these plants derive their thermal energy from the combustion of fossil-fuels and, in doing so, emit large amounts of CO_2 [2]. This CO_2 release is the focus of EU policy and the European Commission's 'Roadmap for moving to a low-carbon economy in 2050' [3] presents the motivations to achieve an 80% reduction in greenhouse gas emissions by 2050.

CO_2 capture and sequestration (CCS) technologies will almost certainly be required in fossil-fuelled thermal power plants to achieve the reductions sought [4]. Three methods of CCS are widely regarded as being suitable for this task: (i) pre-combustion capture; (ii) post-combustion capture; and (iii) combustion in oxygen. All three processes are energy intensive and contribute to a significant reduction in overall plant cycle efficiency [5]. CCS is the

* Corresponding author.
E-mail address: jonathan.siviter@glasgow.ac.uk (J. Siviter).

http://dx.doi.org/10.1016/j.apenergy.2014.11.075
0306-2619/

Nomenclature

ΔT_{Cu}	temperature difference at Copper blocks in contact with the 'hot' and 'cold' surfaces of a thermoelectric heat pump
Δt	time (in seconds)
ΔT_w	temperature difference of water at the inlet and outlet of the water block
ΔT_{THP}	temperature difference between the 'hot' and 'cold' sides of the thermoelectric heat pump
$\dot{m}$	mass flow (kg/s)
$\dot{P}_{THP}$	electrical power supplied to the thermoelectric heat pump ($W_{e,electrical}$)
AC	Alternating Current
C_p	specific heat capacity at constant pressure
CAD	Computer Aided Design
CAPEX	Capital Expenditure
CCS	CO_2 Capture and Sequestration
$COP_{h,c}$	Coefficient Of Performance of heating or cooling
DC	Direct Current
$I_{max,opt}$	maximum and optimum currents applied to the thermoelectric heat pump (A)
IGCC	Integrate Gasification Combined Cycle
ORC	Organic Rankine Cycle
PCCC	Post Combustion CO_2 Capture
PID	Proportional Integral Derivative
PSU	Power Supply Unit
PWM	Pulse Width Modulation
Q_C	thermal energy absorbed by the 'cold' side of the thermoelectric heat pump ($W_{th,thermal}$)
Q_H	thermal energy generated by the 'hot' side of the thermoelectric heat pump ($W_{th,thermal}$)
TE	Thermoelectric
TEC	Thermoelectric Cooler
TEG	Thermoelectric Generator
THP	Thermoelectric Heat Pump
V_{max}	maximum applied voltage to the thermoelectric heat pump

primary technology necessary to meet present and future energy demands at acceptable carbon emission levels, however, other improvements in the thermal power plant must also be made to limit increasing costs [6]. Beer [7] examines the impact of reducing CO_2 emissions from thermal power plants and the associated penalties each of the various configurations introduce; these are summarised in Table 1.

The Carnot cycle describes the theoretical relationship between the temperature difference in the heat process and the maximum amount of work that can be extracted from the process [8]. The reduced efficiency of the Rankine cycle with respect to the Carnot cycle is a consequence of the lower average temperature of the heat input to the Rankine cycle. The Rankine cycle is always below this limiting condition due irreversibilities and losses inherent in the physical realisation of the process. However, the absolute electrical output and thermal efficiency of a Rankine cycle power plant can still be improved in a number of ways. Examples include varying the steam inlet pressure and temperature [9] and lowering the condenser pressure [10]. From a commercial perspective there is also the economic cost of cycle enhancements to be considered. A recent study of plant located in China [11] concluded that cost efficiency improvements are a significant driver in plant development and the reduction of CO_2 emissions. Similarly, the use of reheat cycles to increase the practically attainable efficiency is well documented [12,13], and investigation of the performance losses attributable to the cooling circuit directly impacts the up-time and availability of the plant [14].

The most commonly used heat transport fluid in the conventional Rankine cycle is pure H_20 for high temperature plant; for lower temperature or low-grade thermal sources organic fluids with a much lower boiling point may be substituted and are frequently referred to as Organic Rankine Cycles (ORC). Efficiency improvements can be achieved by applying the ORC to the plant in specific locations where energy is lost to the environment – so-called "bottoming cycles" – and these have been extensively investigated [15–21]. All, to a greater or less extent, improve the intrinsic cycle efficiency but at a financial cost.

Table 1
Summary of the impact on cycle efficiency of various CCS configurations.

	Subcritical plant	Supercritical plant	(*i*) IGCC	(*ii*) PCC	(*iii*) Oxycombustion
Cycle efficiency	34.3%	43.4%	31.2%	34.1%	30.6%

1.1. Heat pumps

Conventional heat pumps have been previously identified as a technology that can potentially aid the reduction in CO_2 emissions, while improving the net efficiency of energy intensive processes [22–25]. Further, there have been several applications of heat pumps in the literature of THP's replacing conventional heat pumps for air conditioning and refrigeration applications [26–28]. However, to date, little is available in the literature which considers the use of condenser heat pumps as an alternative to bottoming cycles and the authors are not aware of any investigations published which examine the use of thermoelectric heat pumps in this role.

Thermoelectric modules consist of *n*- and *p*-type semiconductors arranged in usually square arrays that can be used in two different ways: in heat pumping mode they utilise the flow of an electrical current through the module to produce a thermal gradient according to the Peltier effect, while in power generating mode they generate an electrical current in an external circuit from an imposed temperature difference, exploiting the Seebeck effect [29,30]. In the latter case they are usually referred to as thermoelectric generators (TEGs) and for the former, as thermoelectric heat pumps (THPs). The coefficient of performance in heating mode, COP_h, where the electrical input power is transported to the 'hot' side of the device is defined as the ratio of heat pumped (Q_H) to power input ($\dot{P}_{THP}$), and is expressed in Eq. (1).

$$COP_h = \frac{Q_H}{\dot{P}_{THP}}; \quad COP_c = \frac{Q_C}{\dot{P}_{THP}} \tag{1}$$

Thermoelectric devices do not use any harmful refrigerants, have no moving parts, are electrically and mechanically robust, are silent in operation and have a high inherent reliability [31]. These attributes make them an attractive option for power plant use where continuous service is a primary consideration.

Thermoelectric devices have been applied to refrigeration cycles [32] and some investigation of their application to electrical power generation in thermal power plants has been conducted [33–35]. However, for power generation from waste heat the output obtained is either so low as to be unviable, or their use has resulted in a net decrease of the overall plant efficiency, due principally to the low thermal to electrical conversion efficiency of the TEGs.

Knox et al. [36] proposed to use thermoelectric devices in heat pumping mode inside the condenser. They also quantified the potential benefits achievable [37], when considering a 600 MW_e generating set in a 44.9% efficient thermal power plant. By the addition of a THP system with an overall COP_h of 3 in the plant condenser a 0.4% increase in cycle efficiency and a 3% reduction in fuel supplied to the boiler was achievable.

This paper extends the previous work and presents results for commercial THPs intended for the condenser application described by Knox et al. By combining the theoretical model and experimental results the practicality of their application is assessed. The findings lead to the conclusion that savings in fuel costs and CO_2 emissions are quite feasible and economically attractive to the plant operator.

2. Thermoelectric heat pump (THP) theory

Thermoelectric heat pump operation depends principally on the Peltier effect: as electrical power is applied to the *n*- and *p*-couples it causes the movement of charge carriers, driving heat transfer through phonon transport. As the temperature difference across the device increases, the Seebeck effect has an increasingly significant role in producing an EMF that acts to counter the applied voltage, leading to reduced current flow. Due to the electrical resistance of the semiconductor material, Joule heating is also present, being proportional to the square of the current flowing in the device. In order to assess the thermoelectric device performance limits, the maximum heat flux and efficiency of converting electrical power to thermal energy transport are measured. Prior work [32,38] has shown the impact that the pellets' cross-sectional area and length have on the cooling performance. For heat pumping, pellets with large cross sectional area (>5 mm^2) and short to medium length (<5 mm^2) are preferred. A commercially available THP was selected for the experimental validation presented in this paper.[1]

The diagram in Fig. 1 details the common notation used in the paper for both device and system experimental work. Q_H is the thermal energy removed at the 'heated' side, Q_c is the thermal input power resulting from the energy supplied by electrical heaters in the experiments in Section 3 or alternatively the latent heat of condensation in the experimental Rankine cycle apparatus described in Section 4. $\dot{P}_{THP}$ is the electrical power applied to the thermoelectric heat pump.

The application of a thermoelectric heat pump to the Rankine cycle establishes an increase in feed water temperature (ΔT_w) returning from the condenser to the boiler. The modified cycle is shown schematically in Fig. 8 in Section 5.1 where the revised physical layout is discussed in detail. This is achieved by passing the feedwater over the 'heated' side of the device. Use of THPs for this type of application is now well established. Previous work [39] has investigated the optimal pellet length and cross-sectional area for a TE device applied as a cooler to achieve the maximum cooling power. Phelan et al. [40] investigated the impact of the thermal resistance on the COP of cooling for a THP, especially if the heat transfer medium is air and this is further emphasised by David et al. [41] investigating the impact different designs of micro-channel heat exchanger have on the COP_c of cooling. Their study found that there is a trade-off between thermal output power and COP_c whereby optimising the heat exchanger design for maximum COP_c leads to a low value of thermal power generated by the THP. A 30% improvement [42] in thermal energy

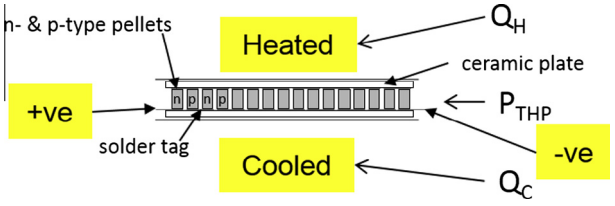

Fig. 1. Thermoelectric heat pump showing the applied power and direction of heat flow.

absorbed by the THP when a liquid is used instead of forced convection when cooling a CPU in a computer has been reported. However, care must be taken when electrically driving the THP as an input power greater than $0.8I_{max}$ will lead to a temperature increase at the heat absorbing side due to Joule heating [43], where I_{max} is the input current at which the maximum ΔT_{THP} is established across the device.

3. Experimental characterisation of thermoelectric heat pump performance

The apparatus used for testing a single thermoelectric device is shown in Fig. 2. With reference to Fig. 2, each thermocouple and the pressure transducer (a load cell) used are denoted by 'T' and 'P' respectively. The system configuration is derived from previous work that characterised the performance of thermoelectric generators [44]. A data-logging unit is used to interface the various transducers used in the experimental apparatus to the computer. An automated program, written in Agilent VEE Pro, measures and records temperature and electrical readings from the heat source and the thermoelectric heat pump. This program also implements various control and feedback functions.

A variable speed gear pump is used to circulate water from a storage tank to the heat removal side of the system. Water temperature is held constant by the use of an in-line chiller unit with an accuracy of ±0.1 °C. In order to maintain a constant pressure on the thermoelectric module to accommodate variable thermal expansion effects, mechanical compliance is provided by a compression spring in the clamping arrangement for the device. A stepper motor is used to adjust the spring's preload and control of the set point is via a load cell and software feedback loop to the stepper controller. The use of a stepper motor enabled extremely accurate control of the pressure between the surfaces of the THP's and the heat sink faces. As the device experienced thermal contraction and expansion the stepper motor adjusted the pressure to ensure optimal pressure conditions defined by the manufacturer of 1.25 MPa[2] were maintained. The heat source in the apparatus comprises of a copper block containing two Silicon Nitride electrical heaters operated in parallel, each able to provide up to 500 W. Heat source temperature measurement is by the use of three thermocouples – one at the thermoelectric device ceramic face in contact with the hot-side heat sink and the others in contact with the upper face of each of the heaters. A further three thermocouples are used on the heat removal side of the test fixture: one in contact with the THP ceramic face and the other two to measure the inlet and outlet water temperatures of the aluminium labyrinth heat exchanger block. This configuration of test fixture allows the precise measurement of thermal power flow to, through and from the device under test. Thermal losses due to convection and radiation are minimised by insulating the whole fixture using glass fibre and additionally by placing a thin Mica sheet around the exposed thermoelectric pellets on peripheral

[1] The thermoelectric device tested is a European Thermodynamics Ltd ET-127-20-15-RS having dimensions 55 × 55 × 4.6 mm. Ceramic height = 0.3 mm, 0.5 μm in solder and 4 mm pellet length.

[2] For a 50 × 50 mm THP a clamping force of 1.25 MPa equates to 378 kg on a 55 mm dimension thermoelectric device.

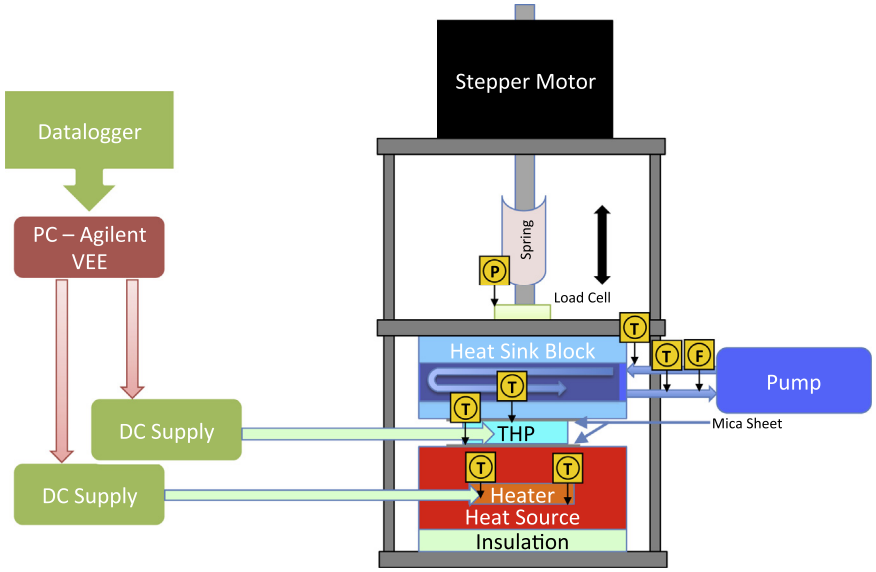

Fig. 2. Test apparatus schematic for the characterisation of a THP.

faces of the THP. This also minimises any effects due to ambient air movement in the vicinity of the test fixture. Thermal conduction is via the thermoelectric device under test; the clamping arrangement ensures there are is minimal heat loss through the clamping apparatus.

The quantity of energy transported from the 'cold' to the 'hot' side is the sum of that converted from electrical to thermal form via the heaters and Q_H. Energy pumped from the cold side is determined by precise measurement of the temperature rise of a known mass flow rate of water. The actual energy provided by the electrical power supply is then subtracted to give Q_H, and shown in Eq. (2).

$$Q_H = \dot{m}Cp\Delta T_{wo-wi} \tag{2}$$

Accurate measurement of the change in water temperature is achieved by the use of the thermocouples placed at the entrance and exit of the aluminium labyrinth heat exchanger. The mass flow rate is determined by the displacement of the gear pump (a specification parameter) and the mechanical RPM of the pump rotor. The Coefficient of Performance (COP heating or cooling) is given by the ratio of the thermal energy to electrical energy (Eq. (1)).

3.1. Determination of the coefficient of performance of heating

As previously noted, the COP_h curve for a THP is determined by a complex and non-linear interaction between the Seebeck and Peltier effects, Joule heating, the amount of thermal energy being pumped and over what temperature range. To obtain the COP_h curve of the thermoelectric device for a given ΔT_{THP} requires that the electrical current applied to it is increased in a series of steps from zero to a value where the peak Q_H has been passed, subject to the constraint that I_{max} is never exceeded. This is repeated for a range of ΔT_{THP}s across the device to obtain a family of curves that describe device performance. The optimum current (I_{opt}) corresponds to the peak value of the COP for the particular ΔT_{THP} under consideration. To obtain a family of COP_h curves for the chosen thermoelectric module the following procedural steps are implemented using the automated control program written in VEE Pro.

(a) All system components are allowed to reach thermal equilibrium at the ambient temperature of the laboratory.
(b) The desired temperature difference across the device under test, the desired mechanical clamping pressure, input electrical current increment and maximum current are all set in the control programme by the user. The programme then calculates the V_{max} of the device and sets the power supply to operate in constant voltage mode.
(c) The instruments are programmed and an initial set of measurements at $\Delta T_{THP} = 0$ (i.e. when the system is still in thermal equilibrium) is taken. These readings are subsequently used to calculate the calibration offset factors for each of the thermocouples used.
(d) The flow rate through the gear pump and the chiller temperature are set.
(e) The control programme then starts incrementing the current applied to the THP.

1. For each increment, the desired temperature across the device is maintained using a software PID control loop by varying the electrical power supplied to the Silicon Nitride heaters. This provides a source of thermal energy at the 'cold' side for the THP to pump to the heated side.
2. The control programme then waits until the temperatures have stabilised at the desired temperature difference (determined by obtaining 5 successive readings within the desired temperature tolerance, each separated by 5 s) and then the programme then records the temperature of each of the heaters, the heatsink surfaces (at Q_H and Q_C), and the water inlet and the water outlet temperatures as shown in Fig. 2.
3. For each measurement taken the ratio of input electrical energy to the resultant thermal power flow to the 'hot' side is determined.
4. The control software calculates the next electrical current value and returns to step (e).

(f) When the maximum device current is reached the test for this particular ΔT_{THP} is complete and the programme saves the recorded data to file.

A typical set of data obtained using this technique is shown in Fig. 3. Error bars are included, based on the known uncertainty in the parameter measurements and indicate a 2% margin in measurement error.

3.1.1. Additional tests at low power

During testing using the water block heat exchanger it was found that, for low values of P_{THP}, accurately determining the increase in Q_H was exceptionally difficult because the temperature

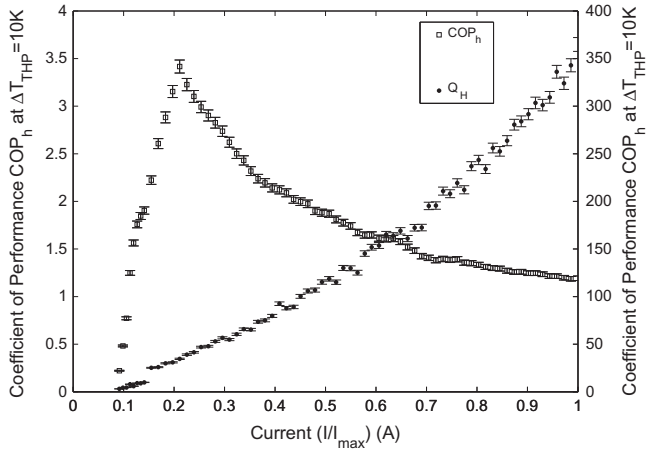

Fig. 3. Performance metrics generated at a temperature difference of 10 °C showing Q_H and COP_h.

difference in the fluid between the input and output of the heated water loop was a few thousandths of a Kelvin, even at low flow rates. This is less than the short-term repeatability of the temperature measurement accuracy of the Agilent data logger, despite using the in-built functions to improve accuracy. In order to facilitate more accurate measurements at low Q_H a supplementary thermal characterisation was undertaken.

For this additional work the temperature change of thermal masses with known specific heat capacities were recorded over a pre-determined time interval. Two blocks of 99.8% pure copper were accurately weighed and the THP then sandwiched between them. The assembly was clamped together using tension springs to provide a compressive force[3] of 0.8 MPa. The whole arrangement was then isolated from ambient temperature fluctuations and drafts by placing it in an insulated box filled with glass fibre. The thermocouples were placed in small diameter holes drilled in the copper blocks, rather than directly on the THP ceramic surfaces as previously. This thermocouple placement gave a greater accuracy in the actual temperature measurement taken and minimised any uncertainty associated with the quality of the thermal contact to the THP ceramic faces. Before experimental data were recorded, a set of measurements was taken to confirm that for small ΔT_{THP}s over a period of 5 min the copper blocks were isothermal to the measurement accuracy of the apparatus. Once this had been established a constant current was applied to the THP in 0.1A increments. For each, the temperature at either side of the THP was recorded at ten second intervals. At low THP power the temperature increase between each measurement is small therefore the increase in temperature between each measurement ($\frac{\Delta T_{Cu}}{\Delta t}$) is calculated over a 60 s interval by post-processing the data after the measurements for a particular current level had completed. The rate of energy increase and decrease at the respective sides of the THP is determined by Eq. (3).

$$Q_H = \frac{mC_p\Delta T_{Cu}}{\Delta t} \tag{3}$$

where m is the mass of the block, C_p is the specific heat capacity and Δt is the time required to change the block temperature by ΔT_{Cu}.

The physical data for the hot-side and cold-side copper blocks are shown in Table 2.

The data obtained by both methods were merged to provide a set of measurements that describe the THP performance over the

Table 2
Data for hot-side and cold-side copper blocks used in low temperature COP_h characterisation.

Copper Specific Heat Capacity	0.39 kJ/kgK
Hot Side Copper Block Dimensions	10 × 10 × 3 cm
Hot Side Copper Block Mass	1.7212 kg
Cold Side Copper Block Dimensions	10 × 10 × 2.9 cm
Cold Side Copper Block Mass	1.6749 kg

temperature and input current ranges of interest. By extracting the COP data at a specific ΔT_{THP} and specific current, the COP_h vs. current curve for each ΔT_{THP} can be obtained for the device tested. An example set of such COP_h curves is shown in Fig. 4.

3.2. Correlation of optimum operating condition by $\frac{I}{I_{max}}$

Both the I_{max} and V_{max} rating of a thermoelectric heat pump are important when defining the highest available COP_h for a given ΔT_{THP}. Where V_{max} and/or I_{max} are applied to the THP the result is the maximum possible ΔT_{THP}. These quantities do not represent the maximum voltages and currents the device can withstand but they are the values that yield the greatest ΔT_{THP} across the device. However, the voltage across the device is directly proportional to the temperature difference (due to the Seebeck effect), and at $I_{max}, Q_H = 0$. The greatest thermal transport occurs at some value less than I_{max}. Therefore, at specific ΔT_{THP}'s in a practical application the optimum operating point will depend principally on the current passing through the device. The coefficient of performance relates the current (or voltage) applied to the THP and the amount of thermal energy pumped. In applications where efficiency (rather than absolute heat pumping capacity) is the primary concern, knowledge of the variation in COP_h is essential. Unfortunately these COP_h curve data are rarely published by device manufacturers and hence are derived from experimental data obtained in the manner described above for the purpose of this study.

Fig. 4 shows that at a particular ΔT_{THP} and low input current the COP_h rises rapidly to a peak value, followed by an exponential decay to unity. Each temperature difference is measured at opposing sides of the THP and Q_H is a function of the increase in water temperature (ΔT_w). At low ΔT_{THP} and low input power the COP_h is higher due to a smaller temperature gradient. As the ΔT_{THP} increases, so the electrical input power must increase and hence the COP_h curve peak moves to the right along the x-axis, corresponding to an increased value of the ratio I:I_{max}. As the I_{max} limit approaches, the COP_h approaches unity as the I^2R losses dominate the thermal performance – energy dissipated in the semiconductor flows equally to each face. Fig. 5 shows the peak COP_h values obtained for each of 4 different ΔT_{THP}s in Fig. 4 and the associated $\frac{I}{I_{max}}$ ratio.

The graphs in Figs. 4 and 5 show that the greatest COP_h available from the heat pump is in the region between $0.1\frac{I}{I_{max}}$ and $0.3\frac{I}{I_{max}}$ where $\frac{I}{I_{max}}$ is the normalised current ratio independent of the maximum heat pumping power achieved in testing. This confirms the basic principle that the attainable COP is inversely proportional to the operating ΔT_{THP} and quantifies the rather vague data provided by device manufacturers, to the measurement accuracy shown in Fig. 5. A best-fit straight line through the data points in Fig. 4 enables a first-order estimate of the COP_h at any intermediate ΔT_{THP}s. More importantly, establishing these data now permits a robust analysis of the actual performance likely to be obtained from commercially available THPs.[4] The scattering of data points below $\frac{I}{I_{max}} = 0.2$ in Fig. 4, especially at low ΔT_{THP}, reflects the great difficulty in repeatably obtaining these data.

[3] The manufacturer's recommendations for clamping pressure for THP modules are provided in [45].

[4] Ferrotec Thermoelectric Modules [46].

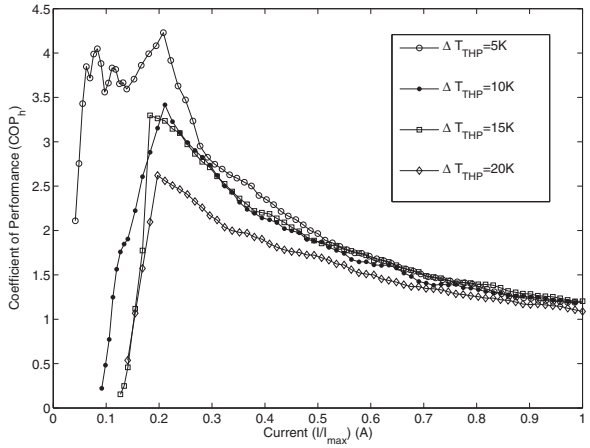

Fig. 4. Coefficient of Performance (heating) for various ΔT_{THP}.

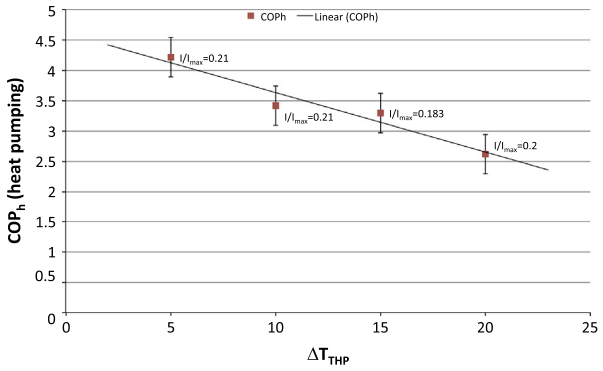

Fig. 5. Greatest COP_h at specific temperature differences and heat pump currents.

4. Impact on plant cycle efficiency

A fundamental requirement for economic use of condenser heat pumping is to ensure that the input power required for the pumping does not exceed the point at which use of the system detracts from overall cycle efficiency. Prior work has determined theoretically that the break-even point above which the heat pump becomes beneficial is when the COP_h exceeds the reciprocal of the cycle efficiency,[5] i.e., $COP_h = \frac{1}{\eta_{cycle}}$.

However, this COP_h threshold calculation does not take into account the temperature at which heat pumping occurs and it is therefore of great interest to determine the largest increase in feedwater temperature returning to the boiler that can be obtained whilst still ensuring that the minimum COP_h requirement is met.

4.1. Cascaded THP arrays

Work presented previously by Knox et al. [37] investigates a three-stage heat pump cascade where the condensate loop exiting the boiler is fed through each stage in series, progressively absorbing the thermal energy transmitted to the hot side of each stage and incrementally increasing the feedwater return temperature. The work explores the theoretical background to the application by detailing the minimum COP_h required to be beneficial to the plant by showing that the reciprocal of the plant efficiency gives the threshold for the application of a THP to be beneficial to the plant in terms of cycle efficiency. Further, the work introduces the concept of cascaded THP arrays, varying the voltage and current at each stage to give the desired increase in thermal energy of the water being pumped back to the boiler.

Fig. 6 shows the implementation of cascaded heat pumps in the condenser. The internal temperature of the condenser remains constant (due to the rejection of latent heat occurring isothermally) at each stage and hence the condensate temperature fedback to the boiler through the THP hot sides must progressively increase to absorb the sensible heat and operate at or above the threshold COP_h. Therefore, each stage of the cascade of heat pumps requires different voltages and currents to be applied for optimum operational efficiency.

4.2. Cascade operating points

Steam in the condenser encounters a 'cooled' side heat sink of the THP. The steam is at low pressure and hence low temperature (nominally 33 °C,45 mbar-abs). Holding the THP below the dew point of the steam forces condensation and hence releases enthalpy which is transported across the heat pump.

In Fig. 6 the heat pump cascade is split into three stages. The temperature of the feedwater increases with each stage and the temperature difference across successive stages also increases. The following conditions are met: $\Delta T_{3w} < \Delta T_{2w} < \Delta T_{1w}$, while for the actual device: $\Delta T_{3THP} > \Delta T_{2THP} > \Delta T_{1THP}$. For each successive stage the attainable COP_h is reduced in comparison with the previous stage, but is still above the theoretical economic minimum as given by Fig. 5.

In order to present a preferential condensation site in the condenser, the'cooled' side temperature of the heat pump must be below that of the ambient steam conditions. For a typical large thermal plant operating at 33 °C/45 mbar-abs a THP cold side of 32 °C is sufficient to achieve this. The aim of the system presented here is to increase the temperature of the water returning to the boiler to 50 °C. This is achieved by increasing the operating temperature difference of the heat pump (ΔT_{THP}) while maintaining the optimum operating conditions (COP_{opt}) obtained from Fig. 5 for that stage, summarised in Table 3.

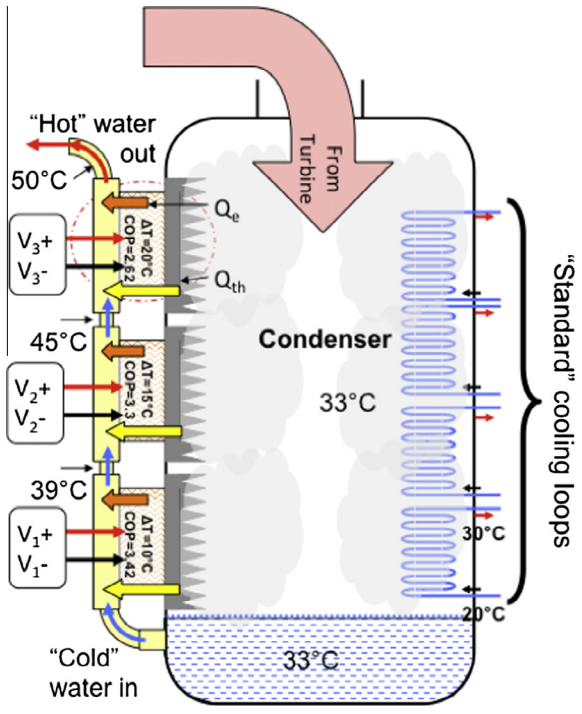

Fig. 6. Triple stage cascaded THP application in the condenser.

[5] $COP_h = 2.2$ for η_{cycle} = 44.9% base cycle efficiency for a typical supercritical plant.

Table 3
Tables (a) and (b) showing the analysis of the THP in the condenser system of Fig. 6.

Stage	T_{Win} (°C)	T_{Wout} (°C)	ΔT (°C)	T_{THPhot} (°C)	$T_{THPcold}$ (°C)	ΔT_{THP} (°C)
(a) Thermal energy analysis at each stage of the THP system						
1	33	39	6	42	32	10
2	39	45	6	47	32	15
3	45	50	5	52	32	20
COP_{opt}		I/I_{max}		Q_H ($\dot{W}_{th}$)		$\dot{m}$ (kg/s)
(b) Coefficient of performance at each stage of the THP system						
3.42		0.21		34.6		0.0013
3.3		0.183		29.9		0.0013
2.62		0.2		28.7		0.0013

With reference the data in Fig. 6, at stage 1 the water enters the base of the THP loop at the condensate exit temperature of 33 °C. In order to achieve a water exit temperature of 39 °C, and using the measured thermal resistance of the heat exchanger of 0.07 °C/W then the required 'heated' side temperature of the THP is 42 °C. Using Fig. 3, for a $\Delta T_{1THP} = 10$ °C the maximum COP_h is 3.42 at $\frac{I}{I_{max}} = 0.21$. Using the modules characterised in this paper, this equates to supplying 10.1 W_e (3.37 V at 3 A), and producing a resultant $Q_H = 34.6$ W_{th}.

At stage 2 water enters at 39 °C and exits at 45 °C giving a required $\Delta T_{2THP} = 15$ °C ($T_{hot} = 47$ °C and $T_{cold} = 32$ °C). At this value, the maximum COP_h is 3.3 at $\frac{I}{I_{max}} = 0.183$. The resultant thermal energy increase to the water feed is 29.9 W_{th} which is achieved by supplying 9 W_e (3.5 V at 2.6 A) to the THP.

For the final stage, the water enters the heat exchanger at 45 °C and increases by 5 °C, exiting at 50 °C. Since the THP_{cold} side remains at 32 °C, the ΔT_{3THP} must be 20 °C in order to achieve the 52 °C required. The optimum COP_h of 2.62 can be obtained by driving the THP at the optimum $\frac{I}{I_{max}} = 0.2$. This gives an equivalent THP input power of 11 W_e (3.9 V at 2.8 A) producing a thermal energy increase to the water of 28.7 W_{th}.

The overall Coefficient of Performance of the cascade averages to 3.11, an electrical power input of 30.1 W_e and an overall increase in thermal power of 93.2 W_{th}. Using these results the potential for scaling up the heat pumping to a real system can now be examined.

5. Physical plant implementation

The heat pump applied to the Rankine cycle requires electrical power and the matter of the source of this power and at what voltage therefore arises. Following the model presented in Section 4, the three-stage cascade can be extended to accommodate much larger heat pumping powers in real plant.

5.1. Electrical requirements

Energy to drive the THP system is an additional parasitic load on the electrical output of the plant. There are many other such loads in the plant – fans, pumps, conveyor systems, etc., and to cater for different load requirements a variety of 3 phase supplies at different voltages are available. In the case of the THP system a DC supply is needed to ensure unidirectional heat pumping in the heat pump modules. Using the data from Section 4, a putative design for the electrical system to power the condenser heat pump system can be considered. The 3 stage cascade system is replicated in parallel to the required extent to provide the energy necessary to raise the feedwater return temperature to 50 °C. The electrical requirements to do this are presented schematically in Fig. 7 and summarised in Table 4.

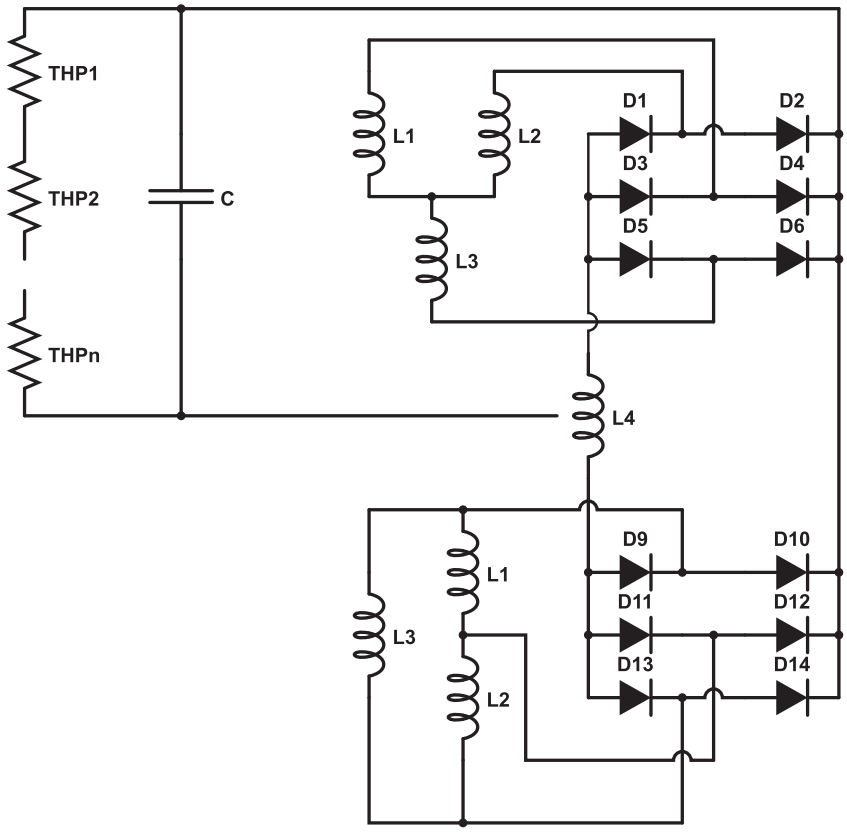

Fig. 7. 12-Pulse AC/DC Rectifier with THP chain.

Table 4
Layout of THP chains and number of devices dependent on the voltage.

Stage	V_{THP}	Devices per chain	Chains required	Total electric power (MW_e)	Total thermal power (MW_{th})
1	3.4	172	1224	2.12	7.21
2	3.6	162	1299	1.9	6.29
3	4	146	1442	2.32	6.04

The paper by Knox et al. [37] notes that for currently available THP technology where the operational COP_h is typically <5 there will be a greater amount of energy available in the condenser from steam condensation than can be economically returned to the feedwater loop. Hence for a large string of devices connected electrically in series (thermally in parallel) the cold sides of the devices are in contact with the same steam conditions throughout the condenser. Work by Montecucco et al. [47] has developed this idea for multiple TEG's to show the effect of series and parallel string configurations has on the output power when subjected to different temperature differences. As the temperature difference across each THP forming one of the stages will be constant, the voltage and internal impedances will be equal, at least to the manufacturing repeatability of the devices, which have performance consistencies of better than 1%. The load current will thus be equal for each device within the same stage and this permits a series/parallel array to be created with convenient electrical drive current and voltage conditions.

With reference to Fig. 7 and for the purpose of this examination, assume a pair of 415 V_{AC} supplies capable of providing 3-phase power is available in the plant from a transformer with outputs 30° apart electrically (a star- and a delta-wound secondary, for example). 415 V_{AC} is preferred over higher voltages, mainly to reduce the electrical insulation requirements and creepage and clearance distances otherwise needed. A 12-pulse rectifier is used to convert the 415 V_{AC} to a nominal 585 V_{DC}. With no output capacitor the ripple voltage is 20 V assuming the conduction angle of each diode pair is 30 degrees. Adding a suitable smoothing capacitor reduces this ripple voltage to 6 V or approximately 1% of the string voltage. This is considered sufficiently 'smooth' for the array of THPs connected to the supply to operate satisfactorily. This DC voltage is supplied to each series-connected chain of thermoelectric heat pump devices.

Many THP chains are connected electrically in parallel array to an individual power supply and are mounted thermally in parallel in the condenser wall. Since each stage of the heat pump cascade operates at a different ΔT_{THP} the voltage across each stage varies and requires a different number of THP's fed from each 415 V_{AC} power pack. Over the large number of devices required there will be a small but significant voltage drop in the wiring required therefore the voltage of each THP is slightly increased, also shown in Table 4. This configuration has the additional benefit of being modular: if a single chain develops a fault, the remaining chains and other cascades can continue to operate unaffected and plant performance is not severely degraded.

Application of such a set of THP arrays to a 600 MW_e Rankine cycle plant that has a feedwater return rate of 273.6 kg/s from the condenser plant is shown in Figs. 8 and 9. In order to meet this mass flow requirement multiple THP arrays will be required. Using the data in Tables 3 and 4, each THP is capable of attaining the desired heat energy transfer at a mass flow of 0.0013 kg/s, therefore a total of 210,462 devices is required. The sum of the electrical powers to the THP is 6.34 MW_e, which is 1.12% of the net electrical output of the plant. Further we can calculate that the large-scale thermal output on the hot side of the THP is 19.54 MW_{th}. Hence the overall coefficient of performance of heating when applied to the plant is 3.11. As previously shown this is above the minimum threshold for the application of a THP to be beneficial to this plant, the threshold being 1/44.9% or 2.22 leading to a new net electrical output of 570.335 MW_e (a reduction of 1.12% required to supply the thermoelectric heat pumps) and a reduction in thermal energy rejected in the condenser of 13.2 MW_{th} (2.29% reduction). This results in a thermal energy value retained by the plant of 19.54 MW_{th}. Hence the new lower fuel consumption rate is 98.48% and therefore the new plant efficiency is 45.05%.

6. Economic justification for inclusion of the THP

The preceding theoretical analysis and experimental results have demonstrated favourable technical operating conditions for

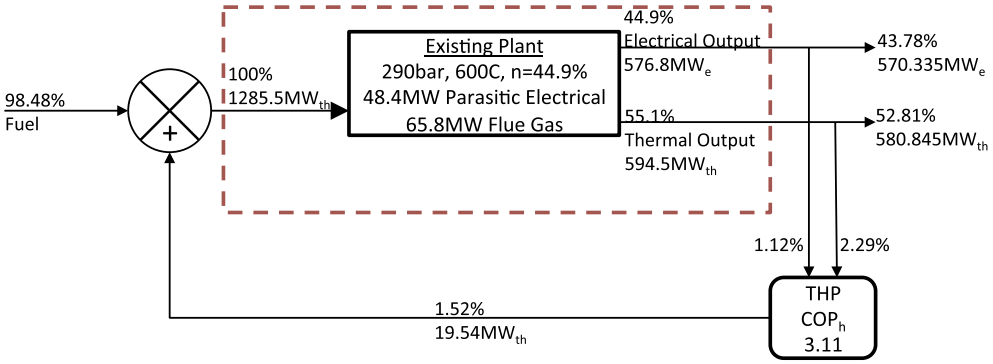

Fig. 8. THP Applied to Rankine plant.

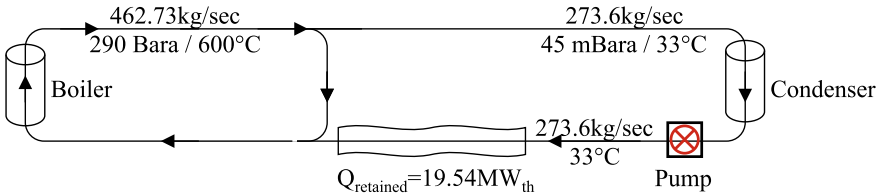

Fig. 9. Application of the THP system to a large scale Rankine plant.

Table 5
Payback period for THP. All figures in millions.

Year	Y0	Y1	Y2	Y3	Y4	Y5
THP system	(12.62)	0	0	0	0	0
Coal reduction	0	5.1	5.1	5.1	5.1	5.1
Electricity revenue	0	(1.89)	(1.89)	(1.89)	(1.89)	(1.89)
Cumulative difference	(12.62)	(9.41)	(6.2)	(2.99)	0.22	3.43

implementing a THP cascade in the Rankine cycle. In order to quantify the economic advantage its impact on a coal-fuelled thermal plant is examined. In the following analysis the additional cost benefit of the reduction in carbon dioxide emissions is excluded for clarity.

6.1. Cost of coal and electricity

Assuming the generating cost of electricity is 3.5 p/kW h and that the plant has load factor of 85% and a capacity of 600 MW_e then a saving of £5.1 million per year can be made the addition of 19.54 MW_{th} of thermal energy to the plant.

If the plant sells electricity at a cost of 4 p/kW h (£40/MW h) then, assuming that 6.334 MW_e is supplied to the THP from the plant, the THP reduces the revenue of the plant by £1.89 million per year.

6.2. Thermal plant equipment CAPEX

For a THP system that consists of 210,462 devices for each stage, it equates to 631,386 devices. Assuming a cost price per THP of £10 then the initial capital cost of only the devices is £6.313 million. The infrastructure and other capital expenditures are estimated at double the cost of the devices, giving a total capital expenditure of £12.62 million. Table 5 shows the interval between the initial capital cost and the payback period, taking into account both the reduced fuel expenditure and lost revenue for decreased sales of kW h of electricity due to the THP system parasitic load. Break-even occurs after a little over 4 years compared with an expected service life of some 30 years for the THP system. This system thus clearly gives a reduced operating cost.

7. Conclusions

Using both experimental evidence and theoretical considerations we have shown that there is scope to improve the cycle efficiency of a thermal power plant using a condenser heat pump system and that today's thermoelectric materials have attained the performance level that makes them a viable technology in this application. More importantly, the THP can be used to reduce the fuel load of the plant through the retention of low grade thermal energy within the overall process; in the above example demonstrating greater than 1.5% reduction in the fuel burnt. Although THPs exhibit a lower COP_h than vapour-compression alternatives, their reliability and simplicity of operation make them a feasible option and in this application the plant fuel load is reduced by 1.52% with a corresponding increase in overall cycle efficiency to 0.15%. Each of the multistage cascade heat pumps is electrically driven to maximise the COP for the required temperature difference across the array devices – of the order of an $\frac{I}{I_{max}}$ratio = 0.2. Heat pumping power densities of the order of 1 MW/m^3 are attainable and their low mass makes them suitable for condenser walls in both retrofit and new designs.

The technical feasibility of using large numbers of thermoelectric heat pumps has been investigated. Each stage of the heat pump cascade requires a different operating voltage and current, therefore there are distinct advantages in using large numbers of devices in parallel arrays and selecting the number of devices in a chain to permit varying drive requirements. Electrical power to control the arrays from 415 $V_{AC}/3\phi$ supplies allows for cost-effective implementation using standard circuitry.

There are numerous other thermoelectric device applications that are become increasingly attractive from an efficiency point-of-view when the rising cost of energy is considered. Therefore, thought must be given to the supply of rare-earth materials used in the production of thermoelectrics, especially when noting that automotive market use is expected to expand very rapidly in the near future. The use of Manganese Silicides as new thermoelectric materials with a high figure-of-merit and found in abundance in the earth's crust are an attractive alternative to Tellurides and are the subject of on-going intense materials research effort as demonstrated by Khan et al. [48] and Mehta et al. [49].

The economic case at the plant level has been examined and, despite the large number of devices, the costs are recoverable in 4 years using a pessimistic estimate of both costs and savings. A more detailed analysis would depend on the particular plant, retrofit vs. new build costs, the prevailing efficiency incentives and subsidies, carbon trading costs, future fuel and Unit selling costs, etc.

A future paper will detail the experimental implementation of a thermoelectric heat pump in a small-scale Rankine cycle apparatus that replicates actual power plant steam conditions and will examine the mechanical implementation required for their successful use.

References

[1] Bugge JR, Kjær S, Blum R. High-efficiency coal-fired power plants development and perspectives. Energy 2006;31(10–11):1437–45. http://dx.doi.org/10.1016/j.energy.2005.05.025. <http://linkinghub.elsevier.com/retrieve/pii/S0360544205001416>.

[2] Yang H, Xu Z, Fan M, Gupta R, Slimane RB, Bland AE, et al. Progress in carbon dioxide separation and capture: a review. J Environ Sci (China) 2008;20(1):14–27. <http://www.ncbi.nlm.nih.gov/pubmed/18572517>.

[3] European Commission. A Roadmap for moving to a competitive low carbon economy in 2050. Tech. rep.; 2011.

[4] Li B, Duan Y, Luebke D, Morreale B. Advances in CO_2 capture technology: a patent review. Appl Energy 2013;102:1439–47. http://dx.doi.org/10.1016/j.apenergy.2012.09.009. <http://linkinghub.elsevier.com/retrieve/pii/S0306261912006496>.

[5] Mondal MK, Balsora HK, Varshney P. Progress and trends in CO^2 capture/separation technologies: a review. Energy 2012;46(1):431–41. http://dx.doi.org/10.1016/j.energy.2012.08.006. <http://linkinghub.elsevier.com/retrieve/pii/S0360544212006184>.

[6] Johansson B. Security aspects of future renewable energy systems – a short overview. Energy 2013;61:598–605. http://dx.doi.org/10.1016/j.energy.2013.09.023. <http://linkinghub.elsevier.com/retrieve/pii/S0360544213007743>.

[7] Beér JM. High efficiency electric power generation: the environmental role. Prog Energy Combust Sci 2007;33(2):107–34. http://dx.doi.org/10.1016/j.pecs.2006.08.002. <http://linkinghub.elsevier.com/retrieve/pii/S0360128506000347>.

[8] Bejan A. Theory of heat transfer-irreversible power plants. Int J Heat Mass Transfer 1995;31(6). <http://www.sciencedirect.com/science/article/pii/0017931088900646>

[9] Geete A, Khandwawala A. Thermodynamic analysis of 120 MW thermal power plant with combined effect of constant inlet pressure (124.61 bar) and different inlet temperatures. Case Stud Therm Eng 2013;1(1):17–25. http://dx.doi.org/10.1016/j.csite.2013.08.001. <http://linkinghub.elsevier.com/retrieve/pii/S2214157X1300004X>.

[10] Wang W, Zeng D, Liu J, Niu Y, Cui C, Feasibility analysis of changing turbine load in power plants using continuous condenser pressure adjustment, Energy. http://dx.doi.org/10.1016/j.energy.2013.11.001, <http://linkinghub.elsevier.com/retrieve/pii/S0360544213009638>.

[11] Wang Y-S, Xie B-C, Shang L-F, Li W-H. Measures to improve the performance of China's thermal power industry in view of cost efficiency. Appl Energy 2013;112:1078–86. http://dx.doi.org/10.1016/j.apenergy.2013.01.037. <http://linkinghub.elsevier.com/retrieve/pii/S0306261913000469>.

[12] Badr O, Probert S, O'Callaghan P. Rankine cycles for steam power-plants. Appl Energy 1990;36(3):191–231. http://dx.doi.org/10.1016/0306-2619(90)90012-3. <http://linkinghub.elsevier.com/retrieve/pii/0306261990900123>.

[13] Yasni E, Carrington C. Off-design exergy audit of a thermal power stations. J Eng Gas Turb Power 1988;110. <http://www.gns.cri.nz/gns/content/download/3872/21478/file/Download3.pdf>

[14] Hoffmann B, Häfele S, Karl U. Analysis of performance losses of thermal power plants in Germany – a system dynamics model approach using data from regional climate modelling. Energy 2013;49:193–203. http://dx.doi.org/10.1016/j.energy.2012.10.034. <http://linkinghub.elsevier.com/retrieve/pii/S0360544212007967>.

[15] Borrnert T. Organic rankine cycle based power plant to utilize low-grade waste heat sources. In: Cement industry technical conference; 2011. p. 1–10.

[16] Angelino G, Invernizzi C, Molteni G. The potential role of organic bottoming Rankine cycles in steam power stations. Proc Inst Mech Eng Part A: J Power Energy 1999;213(2):75–81. http://dx.doi.org/10.1243/0957650991537446. <http://pia.sagepub.com/lookup/doi/10.1243/0957650991537446>.

[17] Murugan RS, Subbarao PMV. Efficiency enhancement in a Rankine cycle power plant: combined cycle approach. Proc Inst Mech Eng Part A: J Power Energy 2008;222(8):753–60. http://dx.doi.org/10.1243/09576509JPE613. <http://pia.sagepub.com/lookup/doi/10.1243/09576509JPE613>.

[18] Wang C, He B, Sun S, Wu Y, Yan N, Yan L, et al. Application of a low pressure economizer for waste heat recovery from the exhaust flue gas in a 600 MW power plant. Energy 2012;48(1):196–202. http://dx.doi.org/10.1016/j.energy.2012.01.045. <http://linkinghub.elsevier.com/retrieve/pii/S0360544212000503>.

[19] Borsukiewicz-Gozdur A. Exergy analysis for maximizing power of organic Rankine cycle power plant driven by open type energy source. Energy 2013;62:73–81. http://dx.doi.org/10.1016/j.energy.2013.03.096. <http://linkinghub.elsevier.com/retrieve/pii/S0360544213003162>.

[20] Mohamed KM, Bettle MC, Gerber AG, Hall JW. Optimization study of large-scale low-grade energy recovery from conventional Rankine cycle power plants. Int J Energy Res 2009;34(12):1071–87. <http://doi.wiley.com/10.1002/er.1629>.

[21] Liu B, Rivière P, Coquelet C, Gicquel R, David F. Investigation of a two stage Rankine cycle for electric power plants. Appl Energy 2012;100:285–94. http://dx.doi.org/10.1016/j.apenergy.2012.05.044. <http://linkinghub.elsevier.com/retrieve/pii/S0306261912004175>.

[22] Neal E. Heat pumps – applications for heating conservation and heat recovery. Prog Energy Combust Sci 1983;9(2).

[23] Byrne P, Miriel J, Lenat Y. Experimental study of an air-source heat pump for simultaneous heating and cooling – part 1: basic concepts and performance verification. Appl Energy 2011;88(5):1841–7. http://dx.doi.org/10.1016/j.apenergy.2010.12.009. <http://linkinghub.elsevier.com/retrieve/pii/S0306261910005167>.

[24] Byrne P, Miriel J, Lenat Y. Experimental study of an air-source heat pump for simultaneous heating and cooling – part 2: dynamic behaviour and two-phase thermosiphon defrosting technique. Appl Energy 2011;88(9):3072–8. http://dx.doi.org/10.1016/j.apenergy.2011.03.002. <http://linkinghub.elsevier.com/retrieve/pii/S0306261911001577>.

[25] Yang S-H, Rhee JY. Utilization and performance evaluation of a surplus air heat pump system for greenhouse cooling and heating. Appl Energy 2013;105:244–51. http://dx.doi.org/10.1016/j.apenergy.2012.12.038. <http://linkinghub.elsevier.com/retrieve/pii/S0306261912009294>.

[26] He W, Zhou J, Hou J, Chen C, Ji J. Theoretical and experimental investigation on a thermoelectric cooling and heating system driven by solar. Appl Energy 2013;107:89–97. http://dx.doi.org/10.1016/j.apenergy.2013.01.055. <http://linkinghub.elsevier.com/retrieve/pii/S0306261913000640>.

[27] Pan Y, Lin B, Chen J. Performance analysis and parametric optimal design of an irreversible multi-couple thermoelectric refrigerator under various operating conditions. Appl Energy 2007;84(9):882–92. http://dx.doi.org/10.1016/j.apenergy.2007.02.008. <http://linkinghub.elsevier.com/retrieve/pii/S0306261907000335>.

[28] Chatterjee S, Pandey K. Thermoelectric cold-chain chests for storing/transporting vaccines in remote regions. Appl Energy 2003;76(4):415–33. http://dx.doi.org/10.1016/S0306-2619(03)00007-2. <http://linkinghub.elsevier.com/retrieve/pii/S0306261903000072>.

[29] Riffat S, Ma X. Thermoelectrics: a review of present and potential applications. Appl Therm Eng 2003;23(8):913–35. http://dx.doi.org/10.1016/S1359-4311(03)00012-7. <http://linkinghub.elsevier.com/retrieve/pii/S1359431103000127>.

[30] Gou X, Xiao H, Yang S. Modeling, experimental study and optimization on low-temperature waste heat thermoelectric generator system. Appl Energy 2010;87(10):3131–6. http://dx.doi.org/10.1016/j.apenergy.2010.02.013. <http://linkinghub.elsevier.com/retrieve/pii/S0306261910000449>.

[31] Rowe D. Applications of nuclear-powered thermoelectric generators in space. Appl Energy 1991;40:241–71. <http://www.sciencedirect.com/science/article/pii/030626199190020X>.

[32] Min G, Rowe D. Experimental evaluation of prototype thermoelectric domestic-refrigerators. Appl Energy 2006;83(2):133–52. http://dx.doi.org/10.1016/j.apenergy.2005.01.002. <http://linkinghub.elsevier.com/retrieve/pii/S0306261905000085>.

[33] Furue T, Hayashida T, Imaizumi Y, Inoue T, Nagao K, Nagai A, et al. Case study on thermoelectric generation system utilizing the exhaust gas of interal-combustion power plant. In: Proceedings ICT 98. XVII International Conference on Thermoelectrics, 1998, vol. 1, 1998, pp. 473–478. <http://ieeexplore.ieee.org/xpl/articleDetails.jsp?arnumber=740421>

[34] Kyono T, Suzuki R, Ono K. Conversion of unused heat energy to electricity by means of thermoelectric generation in condenser. IEEE Trans Energy Convers 2003;18(2):330–4. http://dx.doi.org/10.1109/TEC.2003.811721. <http://ieeexplore.ieee.org/lpdocs/epic03/wrapper.htm?arnumber=1201107>.

[35] Yazawa K, Koh YR, Shakouri A. Optimization of thermoelectric topping combined steam turbine cycles for energy economy. Appl Energy 2013;109:1–9. http://dx.doi.org/10.1016/j.apenergy.2013.03.050. <http://linkinghub.elsevier.com/retrieve/pii/S0306261913002468>.

[36] Knox AR, McCulloch E, Siviter J. Method and apparatus for improvement of efficiency of thermal cycles WO 2012 085551 A2; 2011. <http://patentscope.wipo.int/search/en/WO2012085551>

[37] Knox AR, Buckle J, Siviter J, Montecucco A, McCulloch E. Megawatt-scale application of thermoelectric devices in thermal power plants. J Electron Mater http://dx.doi.org/10.1007/s11664-012-2434-6, <http://link.springer.com/10.1007/s11664-012-2434-6>

[38] Min G, Rowe D. Improved model for calculating the coefficient of performance of a Peltier module. Energy Convers Manage 1999;41:1–9. <http://www.sciencedirect.com/science/article/pii/S0196890499001028>.

[39] Hodes M. Optimal pellet geometries for thermoelectric refrigeration. IEEE Trans Compon Packag Technol 2007;30(1):50–8. http://dx.doi.org/10.1109/TCAPT.2007.892068. <http://ieeexplore.ieee.org/xpls/abs_all.jsp?arnumber=4135393>.

[40] Phelan P, Chiriac V, Lee T. Current and future miniature refrigeration cooling technologies for high power microelectronics. IEEE Trans Compon Packag Technol 2002;25(3):356–65. <http://ieeexplore.ieee.org/xpls/abs_all.jsp?arnumber=1159168>.

[41] David B, Ramousse J, Luo L. Optimization of thermoelectric heat pumps by operating condition management and heat exchanger design. Energy Convers Manage 2012;60:125–33. http://dx.doi.org/10.1016/j.enconman.2012.02.007. <http://linkinghub.elsevier.com/retrieve/pii/S0196890412000611>.

[42] Zhang H, Mui Y, Tarin M. Analysis of thermoelectric cooler performance for high power electronic packages. Appl Therm Eng 2010;30(6-7):561–8. http://dx.doi.org/10.1016/j.applthermaleng.2009.10.020. <http://www.sciencedirect.com/science/article/pii/S1359431109003196>.

[43] Li J, Ma B, Wang R, Han L. Study on a cooling system based on thermoelectric cooler for thermal management of high-power LEDs. Microelectron Reliab 2011;51(12):2210–5. http://dx.doi.org/10.1016/j.microrel.2011.05.006. <http://linkinghub.elsevier.com/retrieve/pii/S0026271411001703>.

[44] Montecucco A, Buckle J, Siviter J, Knox AR. A new test rig for accurate nonparametric measurement and characterization of thermoelectric generators. J Electron Mater 2013;42(7):1966–73. http://dx.doi.org/10.1007/s11664-013-2484-4. <http://link.springer.com/10.1007/s11664-013-2484-4>.

[45] Custom Thermoelectric, Installing a TEG. <http://www.customthermoelectric.com>.

[46] Ferrotec General Purpose Thermoelectric Devices. <https://thermal.ferrotec.com/products/thermal/modules/generalpurpose>.

[47] Montecucco A, Siviter J, Knox AR. The effect of temperature mismatch on thermoelectric generators electrically connected in series and parallel. Appl Energy 2014;123(March):47–54. http://dx.doi.org/10.1016/j.apenergy.2014.02.030. <http://linkinghub.elsevier.com/retrieve/pii/S0306261914001664>.

[48] Khan A, Vlachos N, Kyratsi T. High thermoelectric figure of merit of Mg2Si0.55Sn0.4Ge0.05 materials doped with Bi and Sb. Scripta Mater 2013;69(8):606–9. http://dx.doi.org/10.1016/j.scriptamat.2013.07.008. <http://linkinghub.elsevier.com/retrieve/pii/S1359646213003552>.

[49] Mehta RJ, Zhang Y, Karthik C, Singh B, Siegel RW, Borca-Tasciuc T, et al. A new class of doped nanobulk high-figure-of-merit thermoelectrics by scalable bottom-up assembly. Nat Mater 2012;11(3):233–40. http://dx.doi.org/10.1038/nmat3213. <http://www.ncbi.nlm.nih.gov/pubmed/22231596>.